

Oxides of Nitrogen: N_2O , NO , NO_2



Property data for NO_x are increasingly important to the environmental engineer.

CARL L. YAWS, Texas Instruments Inc.
JACK R. HOPPER, Lamar University

At present, the average U.S. urban concentration of nitrogen oxides* in air is 20–25 times above natural atmospheric conditions [105]. Air-quality standards have been established to combat this alarming increase [112], and consequently many new processing schemes for controlling emissions are under evaluation. Hence, this body of physical property data is especially important for the design engineer.

Critical Properties—Table 3—1

Experimentally determined values for critical temperature, pressure and volume have been determined for all three compounds [1,2,4,9,10,14,17,83,103,118]. The reported values are in close agreement; deviation from the average is less than 1% for critical temperature and volume, and 1.5% for critical pressure.

Vapor Pressure—Fig. 3—1

Extensive vapor-pressure data span the full liquid state for all three oxides. Some data fall below the melting point. In general, agreement is close. Deviations from the least-squares fit are less than 6% in most cases.

Heat of Vaporization—Fig. 3—2

Watson's correlation (Eq. 1—1)[†] is used for expanding heat of vaporization data to cover the full liquid phase.

Heat Capacity—Fig. 3—3, 3—4

The survey of vapor-heat-capacity data shows general agreement with the various literature sources. Average deviation is less than 10% for nitrous oxide and nitrogen

*Nitrogen dioxide data are given for the monomer, NO_2 , only. Any attempt to prepare it results in the formation of an equilibrium mixture of NO_2 and N_2O_4 [4,7]. In the gas phase, the monomer molecules predominate at moderate and high temperatures; at 135°C, the gas is 99% NO_2 [7]. As for the liquid state, nitrogen dioxide molecules are largely dimerized at temperatures below 21.2°C, but the monomer predominates at higher temperatures. At 140°C, the transformation into the monomer is essentially complete. In this paper, gas-phase properties apply only to the NO_2 monomer.

[†]For equations from previous issues, see Part 1, June 10 and Part 2, July 8.

dioxide. Maximum deviation is less than 7% in the case of nitric oxide.

Liquid-heat-capacity data for each oxide have been extended to cover the full liquid state by using the density extrapolation relationship (Eq. 1—3), with $n = 1$. Comparison of the predicted values and experimental data for nitric oxide show fair agreement when extrapolated to temperatures up to 75% of the critical temperature. Average deviation of the extrapolated values is less than 15%.

Density—Fig. 3—5

The generalized correlation of Lu (Eq. 2—2) has been used to extend the laboratory density data over the full liquid state in the cases of nitrous and nitric oxide. For nitrous oxide, a comparison against lab data shows close agreement with a maximum deviation of less than 3%.

Surface Tension—Fig. 3—6

The Othmer relationship (Eq. 1—4) has been used for surface tension over the full liquid range. Comparison of the computed values from the Othmer plot and the experimental data indicate good agreement. Maximum deviation from the least-squares fit is less than 8% for N_2O , 3% for NO , and 5% for NO_2 .

Viscosity—Fig. 3—7, 3—8

Experimental vapor-viscosity data for nitrous and nitric oxides have been extended with tabulated estimates of Svehla [18]. The available experimental data for nitrous oxide have been revised to be representative of the pure component and not of the products of dissociation, which initially occur at about 550°C [122]. The values for nitrogen dioxide have been estimated by the method of Bromley and Wilke (Eq. 2—3). Comparison of the estimates from this method with available experimental data disclose close agreement: Deviations are less than 2% in the case of nitrous oxide and 10% for nitric oxide.

(Text continues on p. 106)

How To Use the Graphs

Each graph is outfitted with a key that lists references and explains just what part of the curve is determined experimentally, and what part is estimated from theoretical correlations.

The shaded squares denote the following:

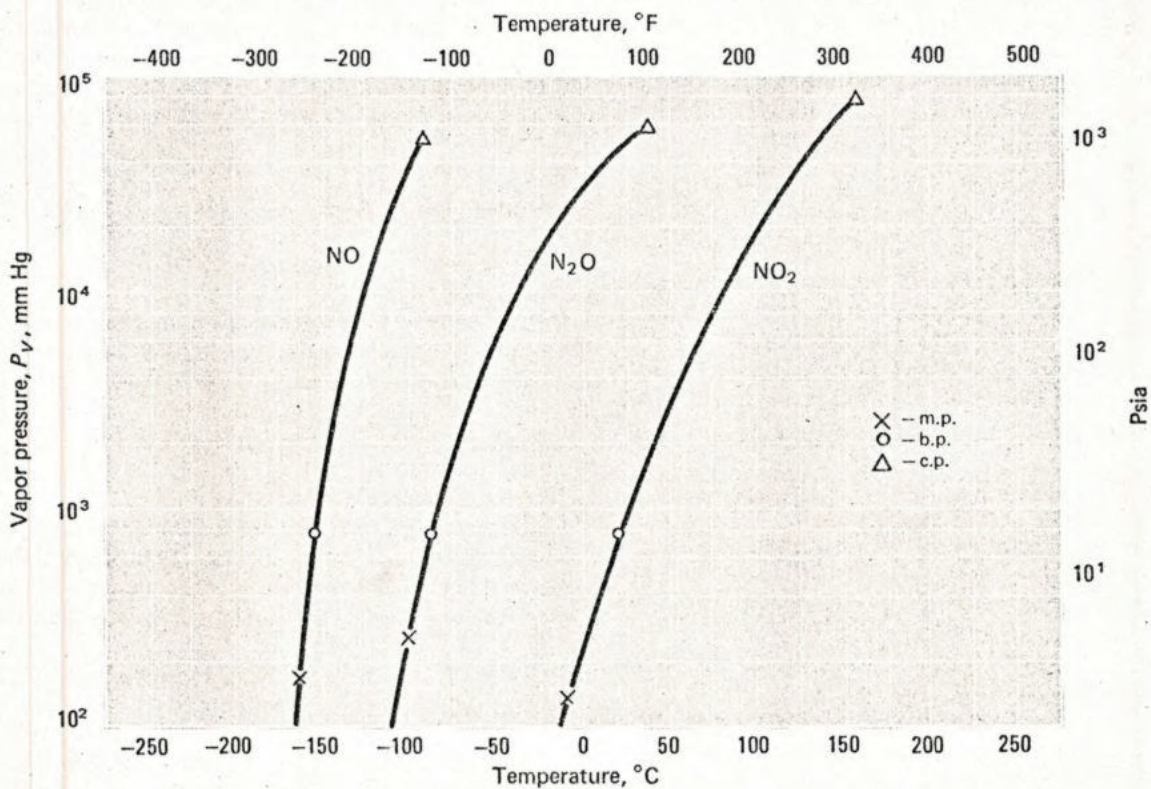
- Data in this region are experimentally known.
- ▣ Experimental and correlated data used.
- All data in this region are correlated.

The "regions" referred to are the temperature ranges between the melting, boiling and critical points (m.p., b.p. and c.p., respectively), or in some cases, the specific temperatures noted in the key.

Physical Properties of the Nitrogen Oxides - Table 3-1

Identification	Nitrous Oxide N ₂ O	Nitric Oxide NO	Nitrogen Dioxide NO ₂
State (std. cond.)	Gas*	Gas*	Gas**
Molecular weight, <i>M</i>	44.01	30.01	46.01
Boiling point, <i>T_b</i> , °C	- 89.5	-151.8	21.2
Melting point, <i>T_m</i> , °C	- 90.8††	-163.8††	-11.2††
	-102.3†		
Critical temp. <i>T_c</i> , °C	36.5	- 93.1	158.0
Critical pressure <i>P_c</i> , atm	71.9	64.4	100.0
Critical volume <i>V_c</i> , cm ³ /gr mol	96.5	57.7	82.2
Critical compressibility factor, <i>Z_c</i>	0.273	0.252	0.232

*colorless. **red-brown. †@ 250 mm. ††@ 760 mm.



Vapor Pressure—Fig. 3-1

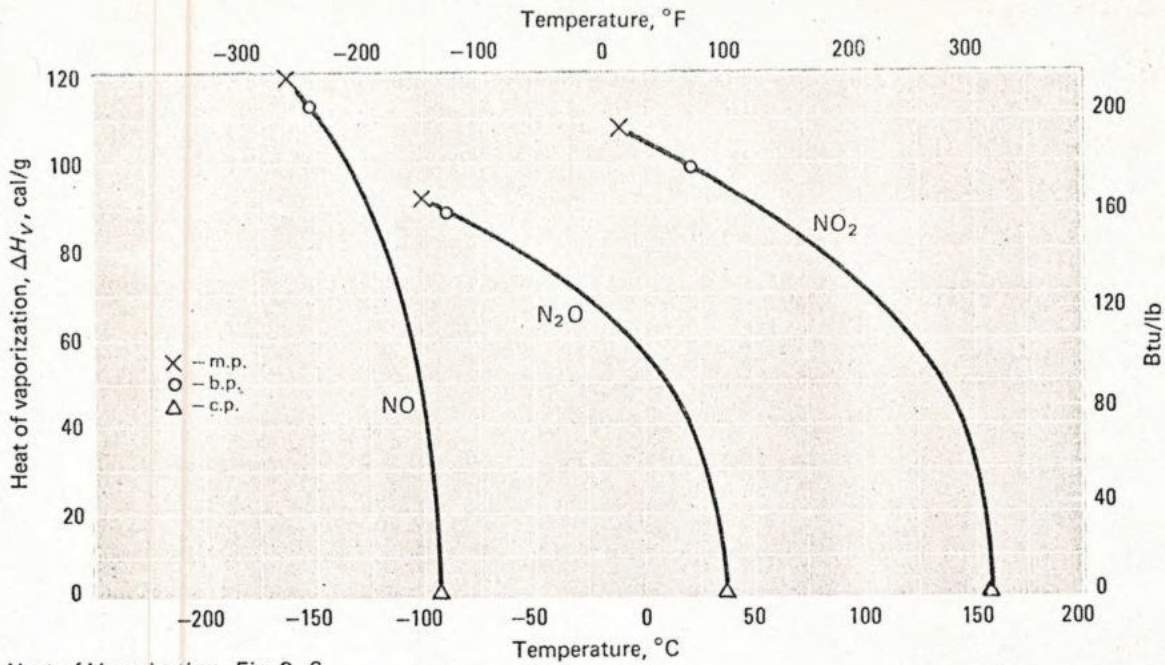
Fig. 3-1	Temperature Range		References
	m.p.-b.p.	b.p.-c.p.	
Nitrous oxide	■	■	1, 2, 5, 10, 12, 13, 17, 87, 103, 104, 110, 118
Nitric oxide	■	■	1, 2, 5, 12, 13, 87, 95, 104, 111, 113
Nitrogen dioxide	■	■	1, 2, 4, 5, 10, 12, 13, 17, 115, 121, 128, 130

■ Laboratory data ▣ Laboratory plus correlations □ All correlated data

Fig. 3-4	Temperature Range		References
	m.p.-b.p.	b.p.-c.p.	
Nitrous oxide	□	▣	19, 100
Nitric oxide	▣	▣	19, 106, 116, 134
Nitrogen dioxide	▣	□	4, 19, 107, 120

■ Laboratory data ▣ Laboratory plus correlations □ All correlated data

Liquid Heat Capacity—Fig. 3-4 →



Heat of Vaporization—Fig. 3-2

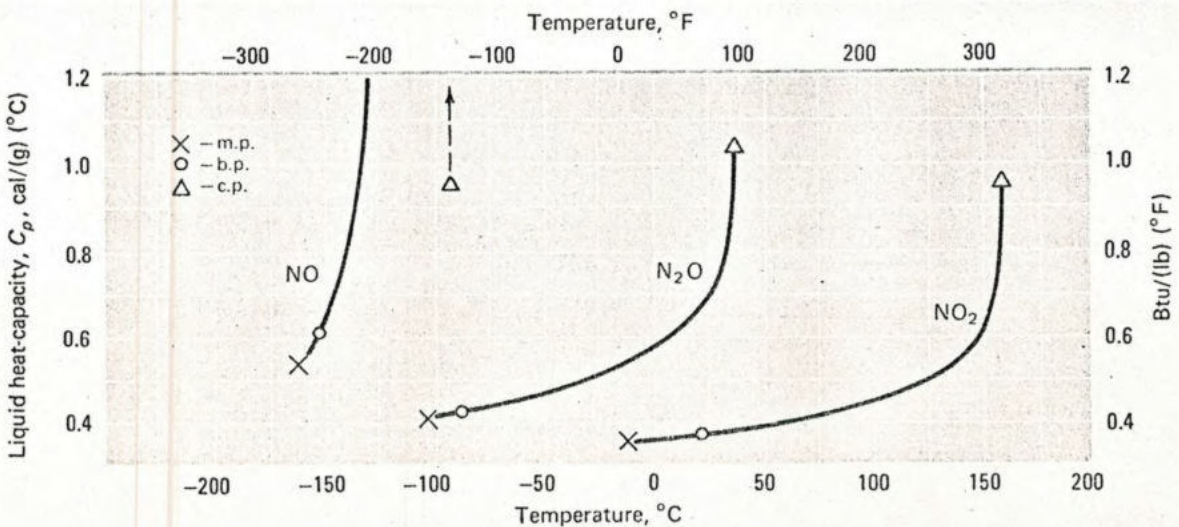
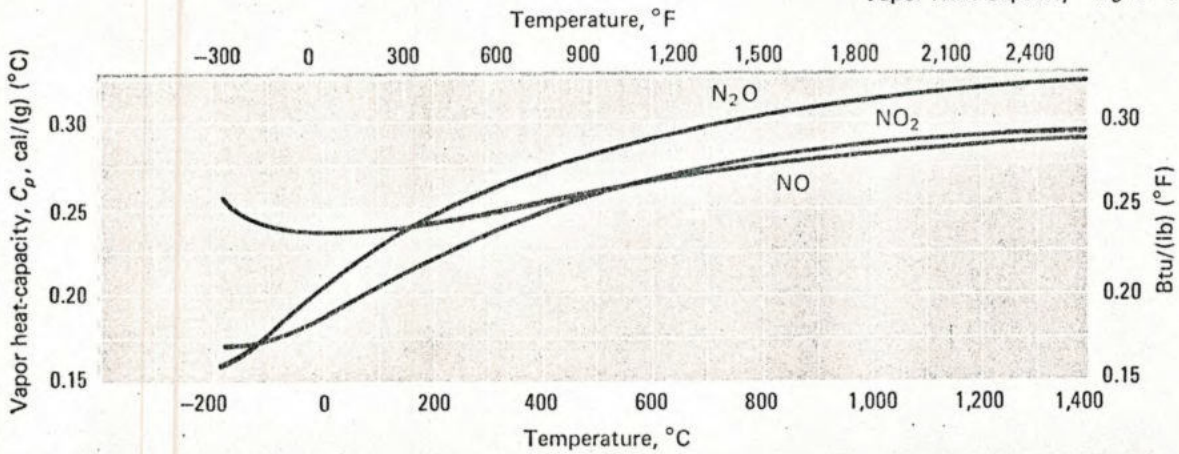
Fig. 3-2	Temperature Range		References
	m.p.-b.p.	b.p.-c.p.	
Nitrous oxide	☑	☑	1, 9, 10, 12, 14, 118
Nitric oxide	☑	☑	1, 9, 10, 12, 14
Nitrogen dioxide	☑	☑	1, 10, 4, 14

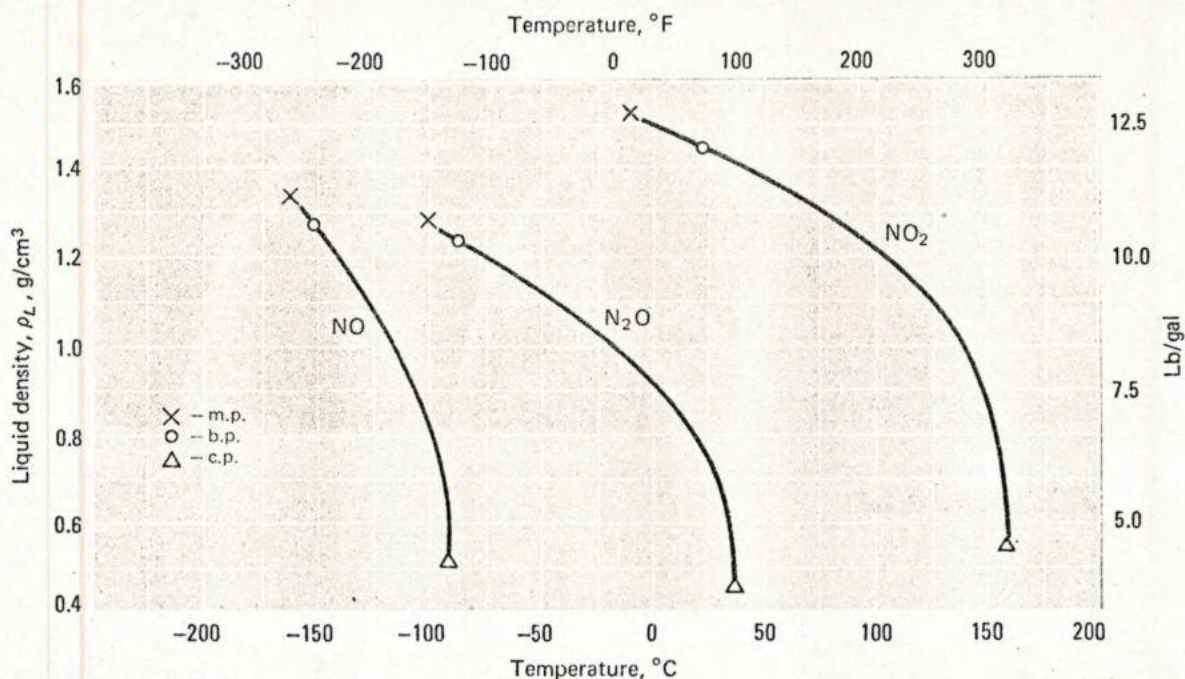
☑ Laboratory data ☑ Laboratory plus correlations ☐ All correlated data

Fig. 3-3	Temperature Range, °C			References
	0-500	500-1,000	1,000-1,500	
Nitrous oxide	☑	☑	☑	7, 8, 10, 15, 19, 21, 117, 119
Nitric oxide	☑	☑	☑	7, 8, 10, 15, 19, 21, 109, 119
Nitrogen dioxide	☑	☑	☑	7, 8, 10, 15, 21, 77, 86

☑ Laboratory data ☑ Laboratory plus correlations ☐ All correlated data

Vapor Heat Capacity—Fig. 3-3





Liquid Density—Fig. 3-5

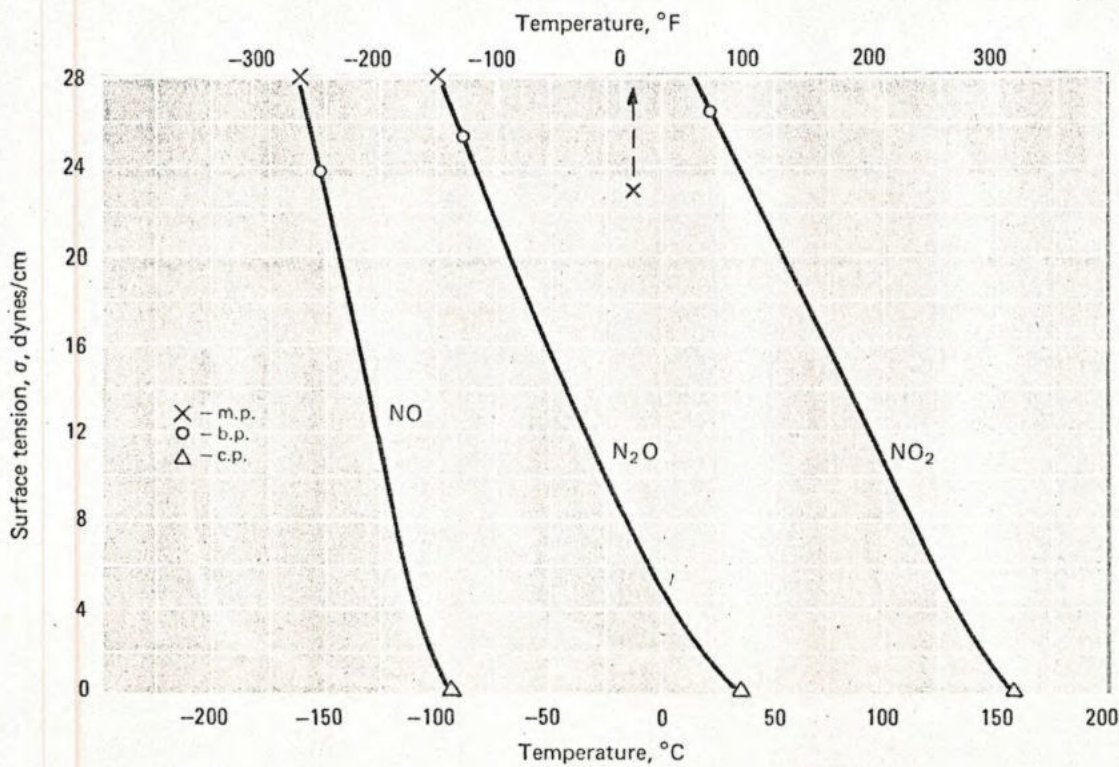
Fig. 3-5	Temperature Range		References
	m.p.-b.p.	b.p.-c.p.	
Nitrous oxide	<input checked="" type="checkbox"/>	<input checked="" type="checkbox"/>	6, 9, 10, 12, 103, 118, 133
Nitric oxide	<input checked="" type="checkbox"/>	<input checked="" type="checkbox"/>	1, 6, 10, 12, 127
Nitrogen dioxide	<input checked="" type="checkbox"/>	<input checked="" type="checkbox"/>	4, 6, 10, 12, 108, 128

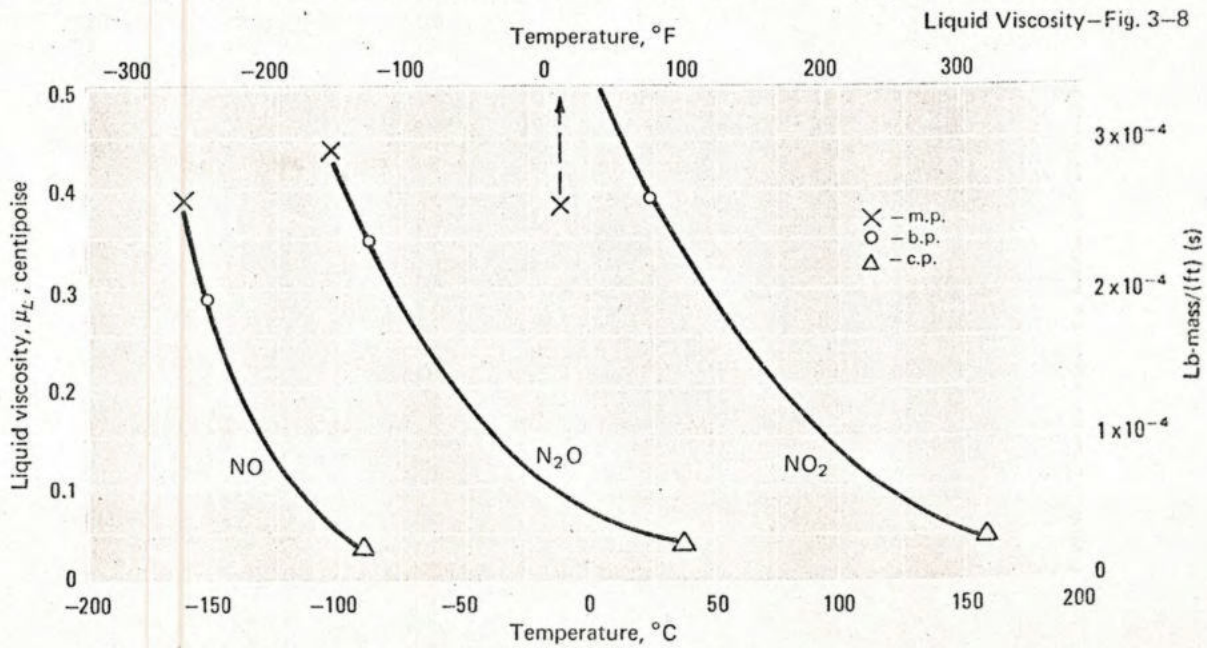
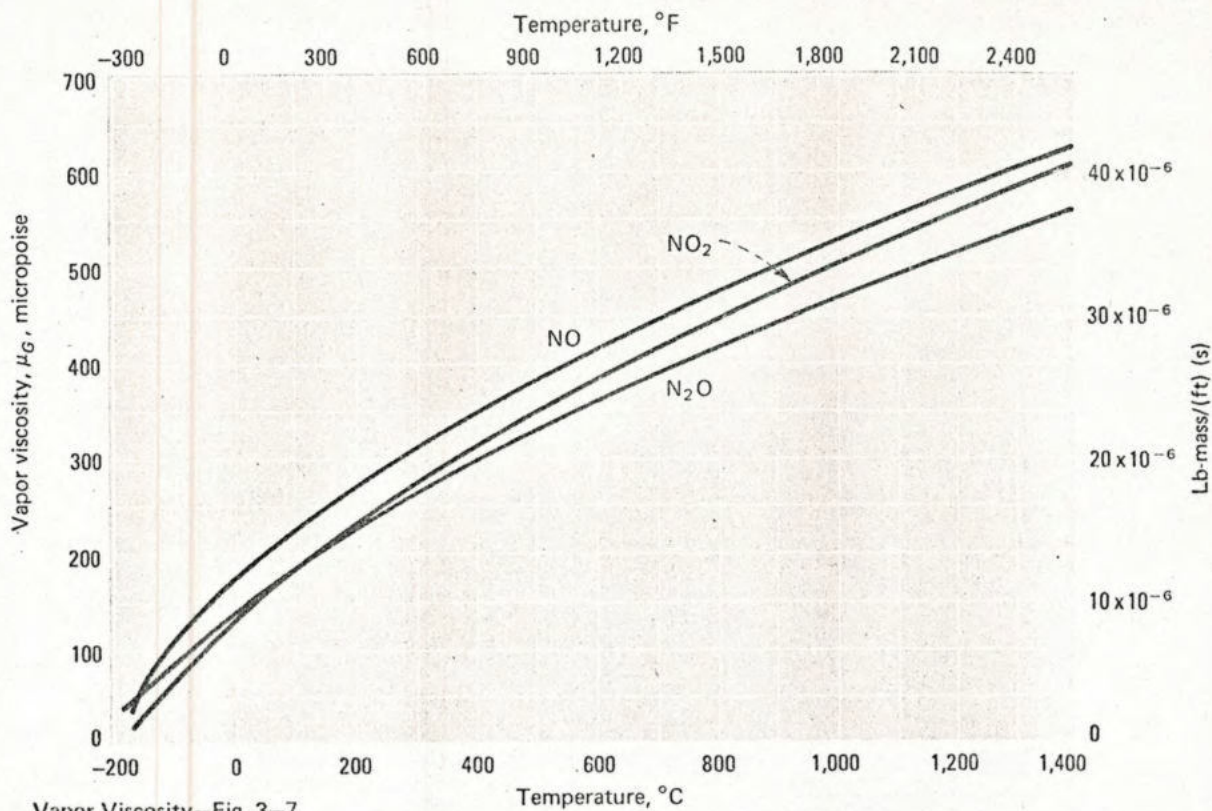
Laboratory data Laboratory plus correlations All correlated data

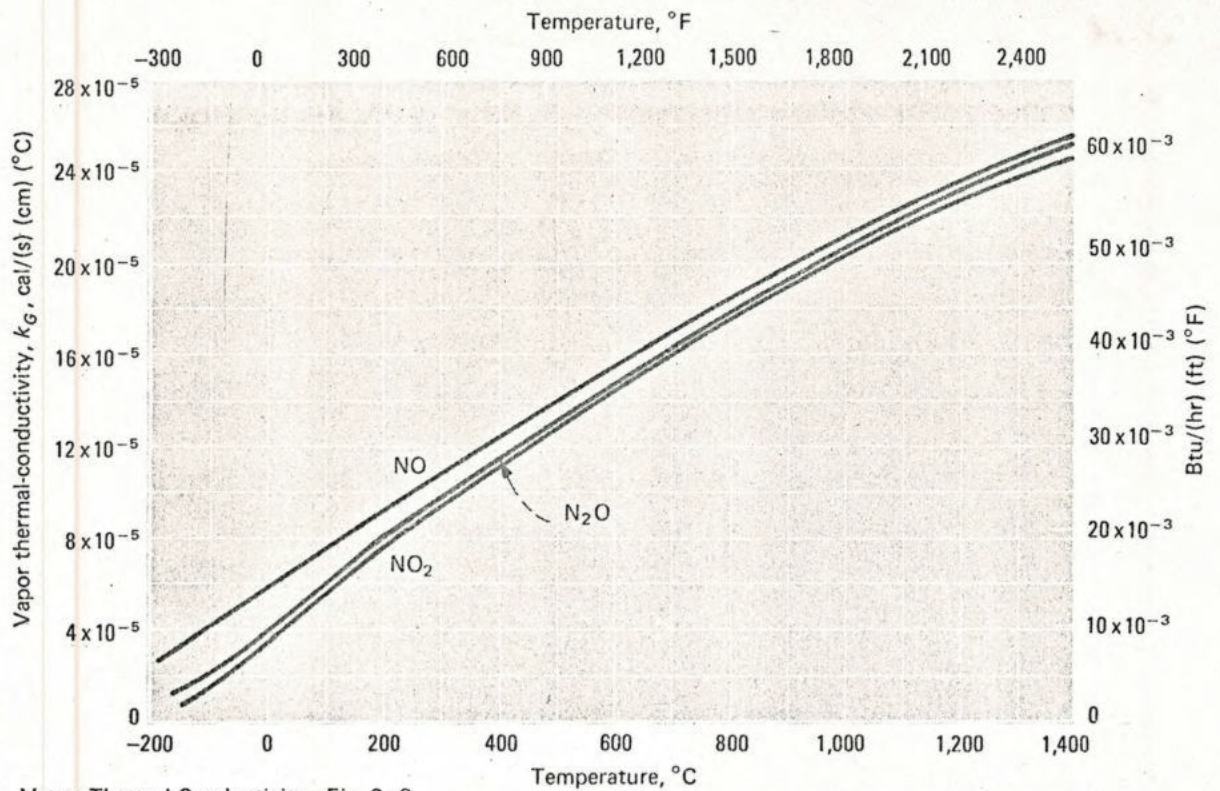
Fig. 3-6	Temperature Range		References
	m.p.-b.p.	b.p.-c.p.	
Nitrous oxide	<input checked="" type="checkbox"/>	<input checked="" type="checkbox"/>	6, 9, 10, 12, 79
Nitric oxide	<input checked="" type="checkbox"/>	<input checked="" type="checkbox"/>	79
Nitrogen dioxide	<input checked="" type="checkbox"/>	<input checked="" type="checkbox"/>	6, 10, 12

Laboratory data Laboratory plus correlations All correlated data

Surface Tension—Fig. 3-6







Vapor Thermal Conductivity—Fig. 3-9

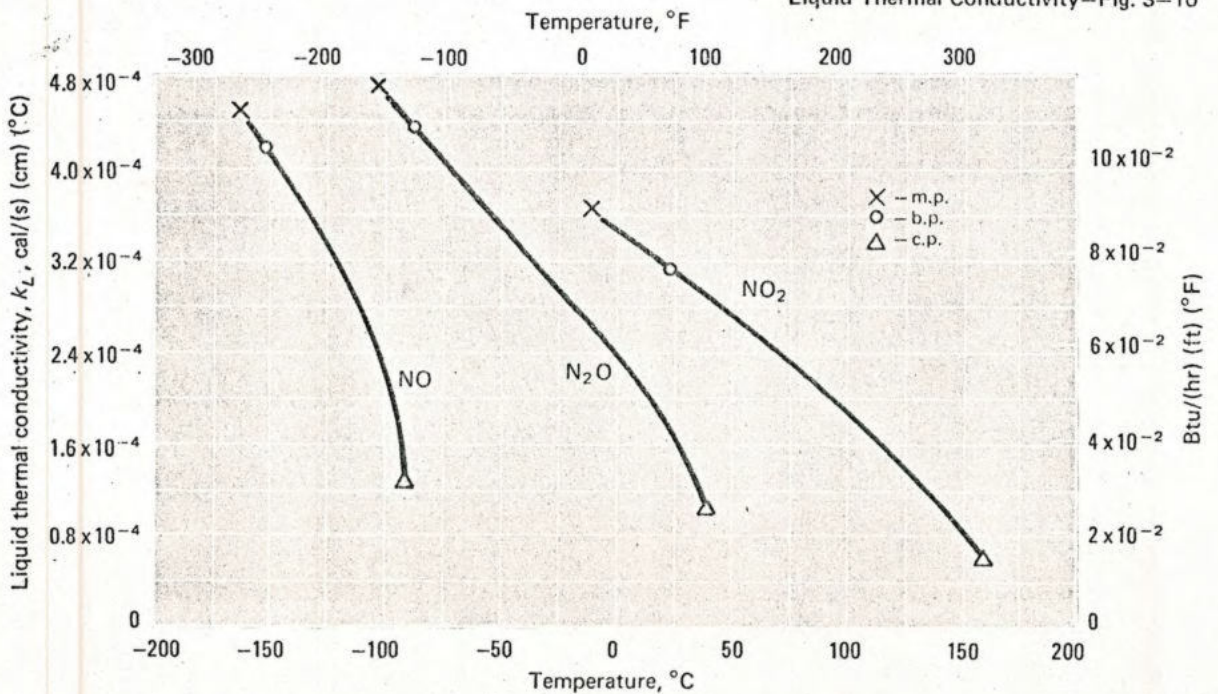
Fig. 3-9	Temperature Range, °C			References
	0-500	500-1,000	1,000-1,500	
Nitrous oxide	<input checked="" type="checkbox"/>	<input checked="" type="checkbox"/>	<input type="checkbox"/>	10, 12, 18, 19, 96, 102, 125, 131
Nitric oxide	<input checked="" type="checkbox"/>	<input type="checkbox"/>	<input type="checkbox"/>	10, 18, 65, 96, 97, 102, 126
Nitrogen dioxide	<input checked="" type="checkbox"/>	<input type="checkbox"/>	<input type="checkbox"/>	10, 12, 98, 99, 101, 132

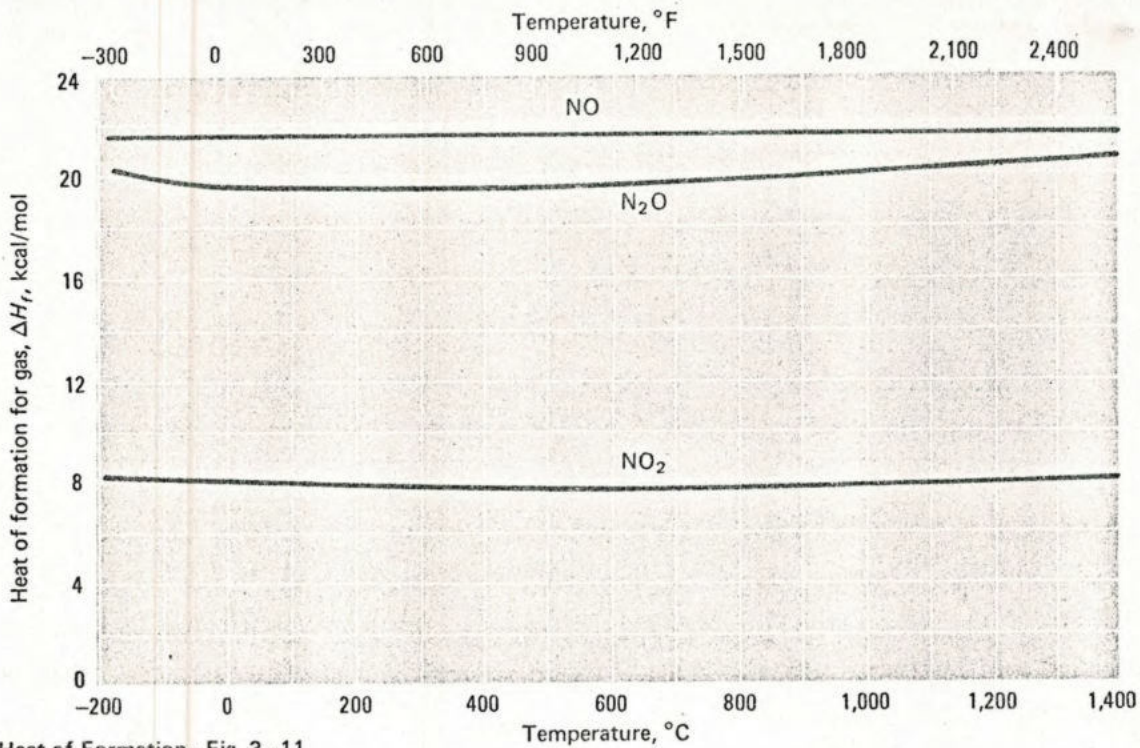
Laboratory data Laboratory plus correlations All correlated data

Fig. 3-10	Temperature Range		References
	m.p.-b.p.	b.p.-c.p.	
Nitrous oxide	<input type="checkbox"/>	<input checked="" type="checkbox"/>	14, 125, 126
Nitric oxide	<input type="checkbox"/>	<input type="checkbox"/>	14, 65
Nitrogen dioxide	<input checked="" type="checkbox"/>	<input checked="" type="checkbox"/>	14, 19

Laboratory data Laboratory plus correlations All correlated data

Liquid Thermal Conductivity—Fig. 3-10





Heat of Formation—Fig. 3-11

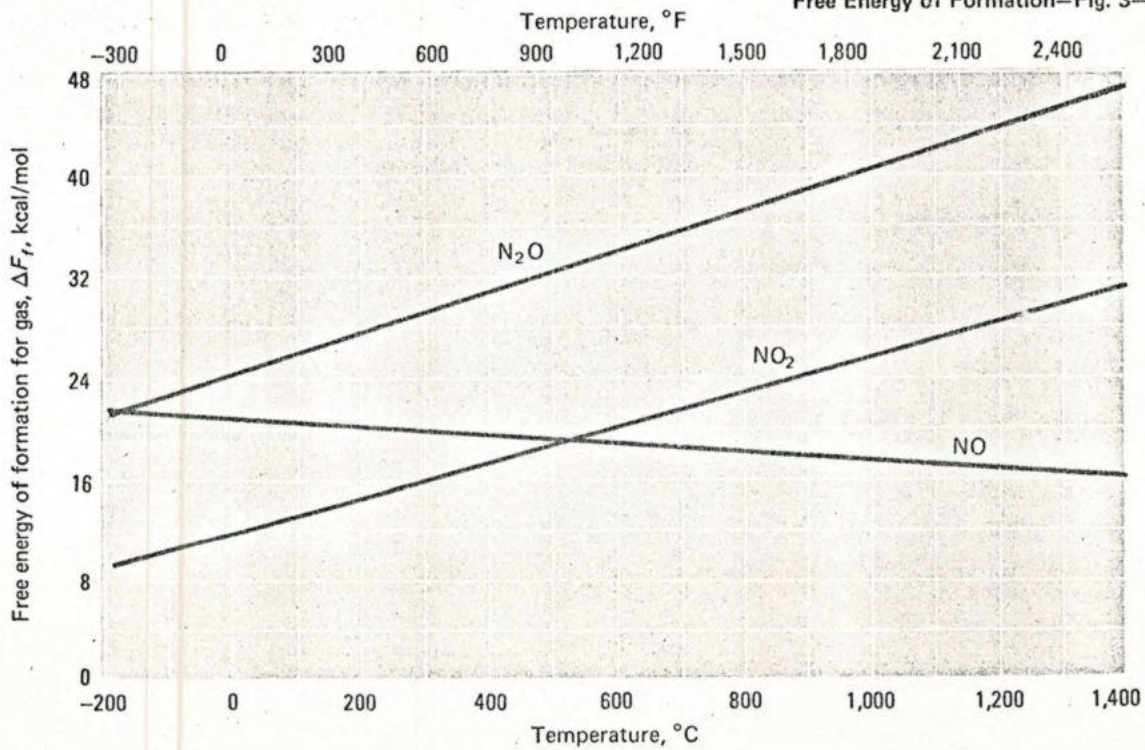
Fig. 3-11	Temperature Range, $^{\circ}\text{C}$			References
	0-500	500-1,000	1,000-1,500	
Nitrous oxide	☑	☑	☑	7, 15, 21
Nitric oxide	☑	☑	☑	7, 15, 21
Nitrogen dioxide	☑	☑	☑	7, 15, 21

☑ Laboratory data ☑ Laboratory plus correlations ☐ All correlated data

Fig. 3-12	Temperature Range, $^{\circ}\text{C}$			References
	0-500	500-1,000	1,000-1,500	
Nitrous oxide	☑	☑	☑	7, 15, 21
Nitric oxide	☑	☑	☑	7, 15, 21
Nitrogen dioxide	☑	☑	☑	7, 15, 21

☑ Laboratory data ☑ Laboratory plus correlations ☐ All correlated data

Free Energy of Formation—Fig. 3-12



OXIDES OF NITROGEN . . .

For nitrogen dioxide, the liquid viscosity was extended over the full liquid state with the Guzman-Andrade equation (Eq. 1-6). Nitrous and nitric oxide values have been estimated by the corresponding states relationship of Stiel and Thodos:

$$\mu_L = \frac{f(Z_c, T_r)}{\xi} \quad (3-1)$$

where μ_L = liquid viscosity in centipoise, and

$$\xi = \frac{T_c^{1/6}}{M^{1/2} P_c^{2/3}}$$

$$T_r = \frac{T}{T_c}$$

The term $f(Z_c, T_r)$ is available from the generalized graphical plot in Reid and Sherwood [14]. Comparison of experimental and predicted values of NO_2 gives order-of-magnitude agreement (average deviation of 55%).

Thermal Conductivity—Fig. 3-9, 3-10

Vapor thermal-conductivity data for nitrogen dioxide were extended beyond the range of experimental determinations from the results of Touloukian et al. [19], which are applicable to a temperature slightly above 1,000°C. Extrapolation gains values for the remaining few hundred degrees.

For nitrous and nitric oxides, the results of Svehla [18] have been used to gain full temperature coverage.

Most of the data from the various sources are in agreement (10% or less deviation), but there are some exceptions. For these, deviations run as high as 26% and 14% for nitrous and nitric oxides, respectively.

Liquid thermal conductivities for nitric oxide were estimated from the corresponding states correlation of Schaefer and Thodos for diatomic gases:

$$k = k_c f(T_r, P_r) \quad (3-2)$$

where $k = k_L$ for saturated liquid. The terms k_c and $f(T_r, P_r)$ are available from the graph in Reid and Sherwood [14].

In the cases of nitrous oxide and nitrogen dioxide, the Stiel and Thodos correlation [14] was modified for liquid-state coverage:

$$(k - k^0) \gamma Z_c^5 = f(\rho_r) \quad (3-3)$$

where:

- k = dense-phase thermal conductivity
- k^0 = low-pressure gas thermal-conductivity
- $\gamma = T_c^{1/6} M^{1/2} / P_c^{2/3}$
- ρ_r = reduced density, ρ / ρ_c .

This modification involved plotting available data (dense gas and liquid phases) of $(k - k^0) \gamma Z_c^5$ versus ρ_r to establish the shape of the correlation curve. Thermal conductivities were then determined from the relation:

$$k_L = f(\rho_r) / \gamma Z_c^5 + k_G \quad (3-4)$$

in which the term $f(\rho_r)$ is available from the correlation curve.

The results from the modified relation are in general

agreement with available experimental data. Average deviations are 3.5% for nitrous oxide, and 17.8% for nitrogen dioxide.

Heat and Free Energy of Formation—Fig. 3-11, 3-12

For these values, several sources give data for the ideal gas, and agreement is within a maximum deviation of less than 1%. One exception is a 5% deviation for the heat of formation of nitrogen dioxide. #

References

References 1-72 are listed in *Chem. Eng.*, June 10, 1974, p. 78; 73-93, July 8, p. 92.

94. Addison, C. C. and Smith, B. C., *J. Chem. Soc.*, 1,783 (1960).
95. Adwentowski, K., *Intern. Bull. Acad. Sci. Cracovie*, **11**, 742 (1909).
96. Barua, A. K. and Mukhopadhyay, P., *Trans. Faraday Soc.*, **63**, 2,379 (1967).
97. Barua, A. K., others, *Int. J. Heat, Mass Transfer*, **12**, 587 (1969).
98. Barua, A. K., others, *Trans. Faraday Soc.*, **65**, 2,913 (1969).
99. Barua, A. K. and Scrivastava, B. H., *J. Chem. Phys.*, **35**, 329 (1961).
100. Blue, R. W. and Giaque, W. F., *J. Am. Chem. Soc.*, **57**, 991 (1935).
101. Brokaw, R. S., NACA, RM E57K19a (1958).
102. Choy, P. and Raw, C. J. G., *J. Chem. Phys.*, **45**, 1,413 (1966).
103. Cook, D., *Trans. Faraday Soc.*, **49**, 716 (1953).
104. Cooper, H. W. and Goldfrank, J. C., *Hydro. Proc.*, **46**, No. 12, 141 (1967).
105. Duprey, R. L., National Center for Pollution Control, Durham, N.C., PHS, No. 99-AP-42, (1968).
106. Eucken, A. and Karwat, E., *Z. Phys. Chem.*, **112**, 467 (1924).
107. Giaque, W. F. and Kemp, J. D., *J. Chem. Phys.*, **6**, 40 (1938).
108. Gray, P. and Rathbone, P., *J. Chem. Soc.*, 3,550 (1958).
109. Gupta, A. D. and Storvick, T. S., *J. Chem. Phys.*, **52**, No. 2, 742 (1970).
110. Hoge, H. J., *J. Res. Nat. Bur. Std.*, **34**, 281 (1945).
111. Hughes, E. E., *J. Chem. Phys.*, **35**, 1,531 (1961).
112. Iammartino, N. R., *Chem. Eng.*, Nov. 26, 1973, p. 24.
113. Johnston, H. L. and Giaque, W. F., *J. Am. Chem. Soc.*, **51**, 3,194 (1929).
114. Joshi, K. M. and Saxena, S. C., *Physica*, **27**, 329 (1961).
115. Kelly, K. K., "The Free Energies of Vaporization and Vapor Pressure of Inorganic Substances," Bur. Mines Bull. 383, Wash., D.C. (1935).
116. Ken, E. C., Univ. Microfilms Publ., 21480 (1929).
117. Kobe, K. A. and Pennington, R. E., *J. Chem. Phys.*, **22**, 1,442 (1954).
118. Kobe, K. A., others, *J. Chem. Eng. Data*, **6**, 229 (1961).
119. Kobe, K. A. and Pennington, R., *Petrol. Refiner*, **29**, 129 (1950).
120. Lewis, B. and Von Elbe, G., *J. Am. Chem. Soc.*, **55**, 511 (1933).
121. Mittasch, A., others, *Z. Anorg. Allgem. Chem.*, **159**, 1 (1926).
122. Raw, C. J. G. and Ellis, C. P., *J. Chem. Phys.*, **28**, 1,198 (1958).
123. Raw, C. J. G. and Ellis, C. P., *J. Chem. Phys.*, **29**, 1,185 (1958).
124. Raw, C. J. G. and Ellis, C. P., *J. Chem. Phys.*, **30**, 574 (1959).
125. Sage, B. H. and Richter, G. H., *J. Chem. Eng. Data*, **8**, No. 2, 221 (1963).
126. Sage, B. H. and Richter, G. H., *J. Chem. Eng. Data*, **4**, No. 1, 36 (1959).
127. Sage, B. H. and Golding, B. J., *Ind. Eng. Chem.*, **43**, 160 (1951).
128. Sage, B. H. and Reamer, H. H., *Ind. Eng. Chem.*, **44**, 185 (1952).
129. Sage, B. H., others, *Ind. Eng. Chem.*, **45**, 2,117 (1953).
130. Sage, B. H. and Schlinger, W. G., *Ind. Eng. Chem.*, **42**, 2,158 (1950).
131. Schramm, B. and Schaefer, K. L., *Ber. Bunsenges. Phys. Chem.*, **69**, 110 (1965).
132. Svehla, R. A. and Brokaw, R. S., *J. Chem. Phys.*, **44**, 4,643 (1966).
133. Taylor, D. J., others, *Can. J. Chem.*, **42**, No. 12, 2,930 (1964).
134. Tsien, H. S., *J. Am. Rocket Soc.*, **23**, 17 (1953).

Meet the Authors

Jack R. Hopper is associate professor of chemical engineering at Lamar University, Beaumont, Tex. He has been associated with Louisiana State University, Exxon Research and Engineering Co., and Humble Oil and Refining Co. His chief research interests are in kinetics, catalysis, process modeling, process control and polymer science. He is currently chairman of the AIChE program committee, Group 1, Area Ib.

Carl L. Yaws—See *Chem. Eng.*, June 10, p. 78, for biography.

